Characterization of Water-Soluble Cellulose Derivatives in Terms of the Molar Mass and Particle Size as well as Their Distribution

W.-M. Kulicke, Christian Clasen, Claudia Lohman*

Institute of Technical and Macromolecular Chemistry, University of Hamburg, Bundesstr. 45, 20146 Hamburg, Germany

Summary: The property profile of cellulose derivatives dissolved in aqueous solvents is not only dependent on the chemical composition (average-, molar- or regiospecific degree of substitution, as well as the substitution along the chain), solvent, temperature and concentration but also on the molar mass and the particle size. All this information can be obtained from the Mark-Houwink-Sakurada-relationship ([η]-M-) or the R_G-M-relationship, if these are at hand. These relationships are suitable for a specific degree of substitution. The R_G-M-relationship has only been determined and published for a few water-soluble cellulose derivatives.
The prerequisite is the availability of a homologous series of samples with the same chemical composition. In this paper it is shown that only the ultrasonic degradation is able to create such a series.
Due to the ability of coupled methods of analysis to acquiring absolute data, molar mass and particle size distributions have been compiled in recent years. Using such methods it was possible to determine molar mass and particle size distributions of several aqueous cellulose derivative solutions by combining a fractionation unit (size exclusion chromatography (SEC) or flow field-flow fractionation (FFFF)) with multi angle laser light scattering (MALLS) for the detection of Mw and R_G and concentration detection (DRI). Results for nonionic cellulose ethers, mixed cellulose ethers, ionic carboxymethyl cellulose, sulfoethyl cellulose, hydrophobically modified hydroxyethyl cellulose were obtained and are partially discussed with focus on the recovery of cellulose derivates after fractionation and the impact on the distribution functions.

Keywords: field flow fractionation; hyphenated techniques; molar mass distribution; size exclusion chromatography; structure-property relations

Introduction

Renewable raw materials (wood, cereals, fats and oils) are gaining considerably in importance because of the constant global demand for energy and raw materials as alternatives to fossil supplies (petroleum, natural gas, coal). The annual world consumption of renewable materials currently totals approx. 6×10^9 t, 3% of the biomass

 DOI: 10.1002/masy.200550511

produced annually.[1] The chemical industry covers approx. 10% of its raw material needs on the basis of renewable materials. In this respect the matrix polysaccharide cellulose acquires enormous significance. Just the annual mass of cellulose formed by photosynthesis is estimated at 10^9-10^{12} t.[2] Of the annual 1.7×10^9 t of timber felled approximately 5% are converted into cellulose by sulphite or sulphate pulping. Of this quantity approx. 5 million t are processed into purified cellulose. As pure cellulose is not soluble in either cold or hot water due to intramolecular hydrogen bonding between the hydroxy groups in position 3 and the ring oxygen atoms of the neighbouring glucose units and intermolecular hydrogen bonds between the 6-hydroxyl groups and the oxygen bonds of the glycosidic linkages, 35% of the purified cellulose is converted to the reaction products cellulose esters (25%) and cellulose ethers (10%).[3]

Unlike pure cellulose, these derivatives maybe water-soluble and are used in a large number of technical applications and products.[4-7] In addition to this, cellulose ethers, because they are physiologically harmless[8] are well-tolerated by the skin and mucous membranes and are therefore used to a great extent in pharmaceutical[9], cosmetic and food products.[10]

A number of parameters have to be taken into account in order to reproducibly adjust the property profile of a cellulose derivative in solution. In addition to the chemical structure and the degrees of substitution it is mainly the molar mass M and solvent depending radius of gyration R_G as well as their distribution that influences the solution properties of a cellulose derivative.

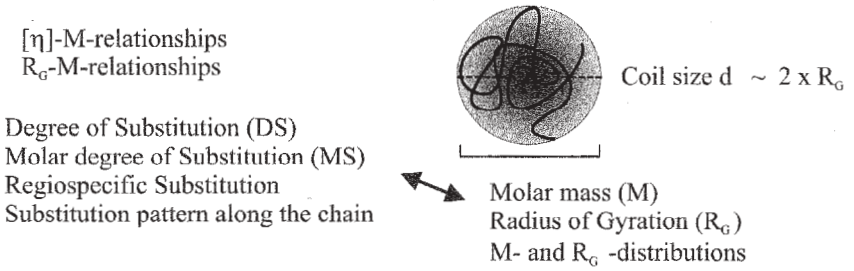

Figure 1. Parameters and relationships influencing the property profile of a single polymer molecule of a cellulose derivative in solution.

Cellulose derivatives can be synthesized in many different ways, but for every value of DS a homologous series of samples is necessary to determine the coils dimensions in solution via [η]-M- and R_G-M-relationships.

This of course also holds for all other chemical variations e.g. the introduction of hydroxyalkyl groups and the creation of a molar degree of substitution.

Therefore one has to search for useful ways of synthesis of homologous series of molar masses with the same chemical composition and structure or to find a general degradation method. On the other hand, if only one native sample is available of high Mw, the only applicable method to obtain a homologous series of molar masses is to degrade the sample in several steps. Several years ago, Kulicke et al. established the ultrasonic degradation for polymer molecules in solution.[11,12] The main advantage of this technique is that the polymer chain breaks in the middle of the chain, no monomers occur during the degradation, and no side chain reactions take place. One aim of this paper is therefore to demonstrate the applicability of this technique to establish the structure-property-relationships for the single molecule and to extend the structure-property-relationships to semi dilute solutions (e.g. η_0-M-c-relationships).

In addition to the average molar mass M and solvent depending radius of gyration R_G, it is especially the distribution function of the molar mass of a cellulose derivative that is of crucial importance for a specific property profile of a technical product as shown in Figure 2. In this case it is not sufficient to characterize the polymer sample with a single average molar mass.

For example the high molar mass tail of the distribution function of a blood plasma volume expander in Figure 2a may lead to an anaphylactic shock. The high molar mass tail in Figure 2a for a methylhydroxyethyl cellulose also determines the relaxation time in extensional flows. The low particle size tail in Figure 2b is responsible for the mechanical stability and dimensional accuracy of the polymeric solid. In Figure 2c the elastic and mechanical as well as the chemical properties are generally enhanced for a more narrow distribution of the molar mass.

To predict and correlate the properties of a distributed polymer sample as the mixed cellulose derivative in Figure 2d used for the mixture, one has to determine this distribution as demonstrated in the second part of this paper with hyphenated techniques as the coupled SEC/MALLS/DRI or FFFF/MALLS/DRI.

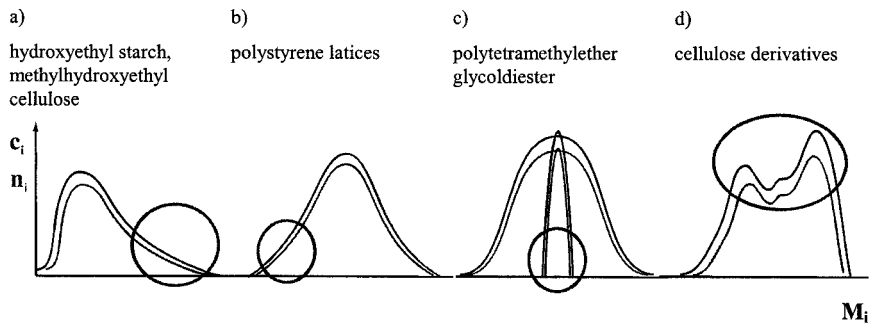

Figure 2. The high molar mass tail of the distribution function in Figure 2a (shown as the concentration c_i and the number density n_i as a function of the molar mass fraction M_i) of hydroxyethyl starch used as blood plasma volume expander[13] may lead to an anaphylactic shock which is life threatening and to a possible accumulation of high molar constituents in the kidneys. The high molar mass tail also dominates the relaxation behaviour of for example methylhydroxyethyl cellulose in extensional flow fields; the low particle size tail of polystyrene latices in Lego bricks in Figure 2b is responsible for the mechanical stability and dimensional accuracy of the polymeric solid. In Figure 2c, for Polytetramethylether glycoldiester used in segmented polyurethanes as a soft segment[14] the elastic and mechanical properties are improved, as well as the chemical properties which are greatly enhanced for a more narrow distribution of the molar mass from M_w/M_n =1,8 to 1,5.[14] In Figure 2d to achieve the same property profile of cellulose derivatives as well as of all other renewable resources, different samples are mixed and may give multimodal distribution.

Experimental

Ultrasonic Degradation[12,15]

Ultrasonic degradation was performed with a Sonifier 450 from Branson Ultrasonic (Danburg, USA), which works with a frequency of 20 kHz. The prepared samples with a volume of 200 ml were placed in a high-sided 400 ml beaker. The beaker was placed in a Haake K F4 ethanol cooling bath (Haake, Berlin) and maintained at 25°C to prevent thermal degradation. After the ultrasonic degradation the samples were centrifuged for one hour at 13,000 rpm in a Hermle Z 383 centrifuge (Hermle Labortechnik, Wehingen) to remove metallic abrasion[15], frozen and then freeze-dried on the BETA 1-1 from Christ of Osterode, Germany.

SEC-MALLS-DRI

A 0.1 M sodium nitrate solution with 200 ppm sodium azide as antibactericide was used as the solvent and eluent. The sodium nitrate solution was prepared with deionized water that had been purified using an active charcoal column and two ion exchange columns

(Adsorber, Universal und Research, Novodirect, Kehl/Rhein). The sodium nitrate (high purity) and the sodium azide were obtained from Merck (Merck eurolab GmbH, Darmstadt). The solvent was filtered using a cellulose nitrate filter (Sartorius, Göttingen, Germany) with a pore size of 0.1 μm.

The eluent was degassed on-line prior to the pump using an ERC 3315a degasser (ERC Inc., Alteglofsheim) and conveyed with a Gynkotek 300C HPLC pump (Gynkotek, Germering) with a flow-rate of 0.513 ml/min. An Anatop filter of pore size 0.02μm (Whatman International Ltd., Maidstone, England) and a pulse damper (Techlab, Erkerode) were connected after the pump. The samples were injected via the HP Series 1100 autosampler (Hewlett Packard). Directly before the columns was a polycarbonate filter with a pore size of 0.8 μm (Nucleopore, Corning Costar, Bodenheim, Germany). The polymer samples were fractionated using four TSK PW_{XL} columns (TosoHaas, Stuttgart, Germany), which were arranged in order of decreasing pore size (TSK G6000PWXL, TSK G5000PWXL, TSK G4000PWXL, TSK G3000PWXL). The SEC columns were kept constant at 25°C with a Techlab Chromatography column heater (Techlab, Erkerode). A DAWN-F light-scattering photometer (Wyatt Technology Corp., Santa Barbara, USA) was used for measuring the scattered light, the source of which was an He-Ne laser (λ = 632.8 nm) with a flow cell made of highly refractive glass (K5, n_g = 1.52064). Concentration measurement was performed with a Shodex RI SE-71 differential refractometer (Showa Denko, Tokyo, Japan). The measured data were recorded on a standard PC with the program *ASTRA 2.11b* and evaluated with the version *ASTRA for Windows 4.73.04* (Wyatt Technology Corp., Santa Barbara, USA).

FFFF-MALLS-DRI[16,17]

The solvent and eluent consisted of a 0.1 M sodium nitrate solution with 200 ppm sodium azide which was conveyed with a pump by Agilent, 1100 series coupled with an integrated degasser. A constant flow was established by a pulse damper (Techlab, Erkerode). For sample application the Agilent Series 1100 auto sampler was used to inject multiple volumes. For further details see.[18]

The fractionation took place in an asymmetrical channel (Wyatt Technology Corp., Santa Barbara, USA) with a trapezoidal cavern created by a thin plastic spacer (width = 250 μm) The channel was made of a stainless steel bottom and a transparent acrylic glass lid. Between lid, bottom and spacer lay a membrane made of regenerated cellulose with a

molecular cut-off of 10 kDa (Wyatt). The channel flow and the cross flow was established and regulated by an Eclipse F (Wyatt).

For the detection of molar masses and the concentration of these molar mass fractions the fractionation unit was coupled with a DAWN-EOS light-scattering photometer (Wyatt) for the measurement of the scattered light, the source being a high-performance photodiode (λ = 690 nm) connected to a flow cell made of highly refractive glass (K5, n_g = 1.52064). The scattered light was simultaneously detected by 14 static angles (22.5° - 147°) surrounding the flow cell. Concentration measurements were performed with an interferometric refractometer Optilab DSP (Wyatt), which followed the light-scattering photometer. The measured data were recorded and evaluated on a standard PC with the program *ASTRA,* version *for Windows 4.73.04* (Wyatt).

Dimensions of Single Polymer Coils in Solution[19]

To determine the dimensions of polymer coils in solution, the easiest way is to determine the intrinsic viscosity [η],

$$[\eta] = \lim_{c \to 0} \frac{\eta_{sp}}{c}, \quad \eta_{sp} = \frac{\eta - \eta_s}{\eta_s} \qquad (1)$$

with η_s as the solution viscosity, η_{sp} as the specific viscosity and c as the concentration. If a relationship between the intrinsic viscosity and the molar mass already exists, one can simply look up this relationship from several handbooks to determine the molar mass.[19,20] The intrinsic viscosity $[\eta]$ of a polymer in a certain solvent can be correlated with the molar mass M:

$$[\eta] = K_{[\eta]} \cdot M^a \qquad (2)$$

In the literature, this dependence is referred to as the $[\eta]$-M-relationship or the Kuhn-Mark-Houwink-Sakurada-relationship (KMHS-relationship). $K_{[\eta]}$ and a are constant for a given solvent and temperature.

In a similar way the intrinsic viscosity is correlated to the radius of gyration R_G via the R_G-M-relationship

$$R_G = K_{R_G} \cdot M^{\nu} \qquad (3)$$

The exponents a or ν are a measure for the solvent quality and therefore for the solution structure of the dissolved polymer The knowledge of $K_{[\eta]}$ and a allows an easy determination of the molar mass of a polymer by measuring the intrinsic viscosity.

For cellulose derivatives, several $[\eta]$-M and R_G-M-relationships have already been published[21] (Table1).

The intrinsic viscosity of a polymer in solution determines the concentration dependent specific viscosity of the dilute solution.

$$\eta_{sp} = c \cdot [\eta] + K_H \cdot (c \cdot [\eta])^2 \quad (4)$$

From this so called Huggins-equation the solvent quality can be extracted from the Huggins coefficient K_H that describes the interactions of the polymer and the solvent in a similar way as the second virial coefficient A_2 of for example osmometric pressure.[19,22] The determination of an $[\eta]$-M or R_G-M-relationships is conducted with a homologous series of polymer samples with different molar masses. To obtain such a series from a single polymer sample, a good method is ultrasonic degradation, that is also used to lower the viscosity of polymer solutions for NMR-spectroscopy.[11]

Table 1. Coefficients K_{RG} and $K_{[\eta]}$ and exponents a and ν of the $[\eta]$-M and R_G-M-relationship (Eq. (2) and (3)) for different cellulose derivatives.

Cellulose derivative	ν / [−]	K_{RG} / [nm]	a / [-]	K_η / [ml/g]
Methyl cellulose	0.55	$4.4 \cdot 10^{-2}$	0.92	$8.0 \cdot 10^{-2}$
Methyl cellulose			0.55	$3.16 \cdot 10^{-1}$
Sulfoethyl cellulose (0,1 M $NaNO_3$)	0.65	$1.2 \cdot 10^{-2}$	1.19	$1.74 \cdot 10^{-4}$
Carboxymethyl cellulose (0,1 M NaCl)	0.53	$5.6 \cdot 10^{-3}$	0.87	$1.11 \cdot 10^{-2}$
Carboxymethyl cellulose (0,1 M NaCl)	0.70	$6.6 \cdot 10^{-3}$		
Carboxymethylcellulose (0,1 M NaCl)			0.91	$1.23 \cdot 10^{-2}$
Carboxymethylsulfoethyl cellulose			0.91	$6.58 \cdot 10^{-3}$
Hydroxyethylsulfoethyl cellulose	0.58	$3.8 \cdot 10^{-2}$	0.80	$2.3 \cdot 10^{-2}$
Hydroxyethyl cellulose	0.59	$2.6 \cdot 10^{-2}$	0.73	$4.1 \cdot 10^{-2}$
Hydroxyethyl cellulose	0.55	$3.3 \cdot 10^{-2}$	0.65	$1.0 \cdot 10^{-2}$
Hydroxyethyl cellulose			0.87	$9.5 \cdot 10^{-3}$
Hydroxypropyl cellulose	0.56	$2.5 \cdot 10^{-2}$	0.68	$4.2 \cdot 10^{-2}$
Hydroxyethylmethyl cellulose	0.53	$3.8 \cdot 10^{-2}$	0.60	$1.7 \cdot 10^{-1}$
Hydroxyethylmethyl cellulose	0.59	$2.6 \cdot 10^{-2}$	0.83	$2.1 \cdot 10^{-2}$
Hydroxyethylethyl cellulose	0.63	$1.4 \cdot 10^{-2}$	0.88	$2.1 \cdot 10^{-2}$
Hydroxyethylethyl cellulose			0.80	$3.7 \cdot 10^{-2}$
Hydroxypropylmethyl cellulose	0.51	$4.7 \cdot 10^{-2}$	0.53	$3.6 \cdot 10^{-1}$
Celluloseacetate			0.60	$2.1 \cdot 10^{-2}$
Cellulosesulfate	0.55	$5.8 \cdot 10^{-2}$		

Ultrasonic Degradation

The degradation of a polymer can be achieved by several means.[23] Nevertheless, a controlled reduction of the molar mass is only possible if no statistical degradation occurs. In principal, a reduction of the molar mass of a polymer is possible by thermal, chemical and mechanical methods and also by enzymatic degradation or by an energy input via radiation. Thermal[24] and chemical degradation[11] (acidic, alkaline and oxidative) are statistical processes that lead to unwanted mono- and oligomers. In addition, they can lead to modifications of the chemical microstructure of the side groups. In contrast, mechanical degradation methods in mills or pebble beds[25], or shear flow[26,27] yield bigger chain segments. However, the degradation in a pebble bed and the degradation in a shear flow field are not very efficient for a controlled reduction of the molar mass. High intensity ultrasound[15] on the other hand is an established and widely used method for the degradation of polymers in solution that does no lead to side chain reactions or to the occurrence of monomeric units during the degradation[12] and was first established in 1993 by Kulicke et al.[15]

Sound waves from an ultrasound generator cause pressure variations in solution. Local pressure differences in the fluid lead to an evaporation of the solvent that forms bubbles of the order of magnitude of up to 100 micrometers. These bubbles collapse with high energy in microseconds, this process is called cavitation.

The collapsing bubbles induce a strong elongational flow field in the solution as shown in Figure 3. These flow fields[11,28-30] and the shock wave of the cavitation[31] tear the polymer molecules apart. The chain breaks in its center of gravity due to the even distribution of the hydrodynamic forces in the elongational flow field.[12,32] Big polymer coils degrade faster due to the larger hydrodynamic interactions with the solvent in the elongational flow field.[33]

The molar mass of a polymer decreases exponentially with time and reaches a nearly constant minimum molar mass as shown in Figure 4 and for a methylhydroxy cellulose in Table 2. Below a certain chain length, the hydrodynamic forces are not high enough to cause a rupture of the polymer chain. The minimum molar mass depends on the type of polymer and on the energy input of the ultrasound.

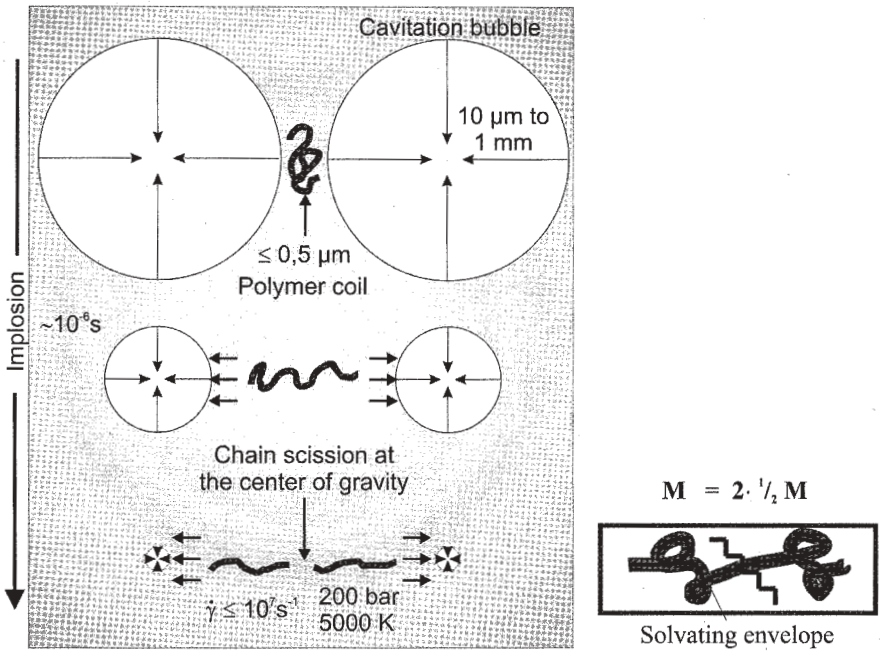

Figure 3. Principle of polymer degradation by elongational stretch between collapsing cavitation bubbles induced by ultrasound. The chain scission always occurs close to the center of gravity of the polymer molecule reduces the molar mass approximately by half for each chain scission.

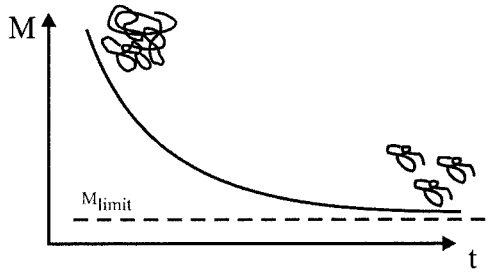

Figure 4. Polymer degradation via ultrasound. The molar mass is reduced to a minimum molar mass, depending on the chemical structure and the energy input.

Spectroscopic detection methods show that the chemical structure of the polymer side groups is not affected by the degradation process. Even large side groups in biopolymers

(for example xanthan gum) stay intact as long as their length is below the minimum length of the polymer backbone.[15] The polydispersity decreases slightly with the time during an ultrasonic degradation, if the original polymer sample had a broad distribution, as can be seen in Table 2.

Table 2. Molar mass as a function of degradation time for a methylhydroxyethyl cellulose.

Irradiation time / min	[η] / cm³/g	M_w/ g/mol	M_w / M_n	$R_{G,z}$ /nm
0	1171	600,000	2.4	94
1	963	390,000	2.4	72
3	644	230,000	1.9	49
5	529	180,000	1.8	42
10	373	120,000	1.7	32
25	217	70,000	1.3	-
60	155	50,000	1.4	-

Structure-Property Relationships

As already indicated by the Huggins-equation (4), the viscosity of a dilute solution of cellulose derivatives directly depends on the concentration c and the coil dimension in form of the intrinsic viscosity $[\eta]$. This also holds for more concentrated solutions, where the polymer coils are already in direct contact with each other. As shown in Figure 5 for a carboxymethyl cellulose, the specific viscosity can be described even for high concentration solely as a function of the product of intrinsic viscosity and concentration. A common ansatz to describe this dependency is with a Taylor series expansion of the Huggins equation (Eq. (4)), where all higher order interactions are combined into a single term, that incorporates the solvent quality exponent a of the Mark-Houwink equation (Eq. (2)):

$$\eta_{sp} = c \cdot [\eta] + K_H \cdot (c \cdot [\eta])^2 + B_n \cdot (c \cdot [\eta])^{\frac{3,4}{a}} \qquad (5)$$

This simple relationship allows an easy determination of the viscosity for a solution of a specific cellulose derivative simply from the concentration and intrinsic viscosity. However, this so called η-$[\eta]$-c-relationship (and in particular the coefficient B_n) has to be determined for each cellulose derivative / solvent system separately. It could be shown for the special case of carboxymethyl cellulose, that in this case the η-$[\eta]$-c-relationships also

hold for varying degrees of substitution for the same cellulose derivative.[34] However, in general the Mark-Houwink relationships are related to the solution structure and therefore sensitive to the substitution patterns, so the intrinsic viscosity will vary for a constant molar mass with the substitution pattern.

These structure-property-relationships allow the extraction of an important critical value for a solution, the critical concentration. At this concentration, the solution is filled with polymer coils and the coils start to interpenetrate and lead to the steep increase of the solution viscosity as seen in Figure 5.

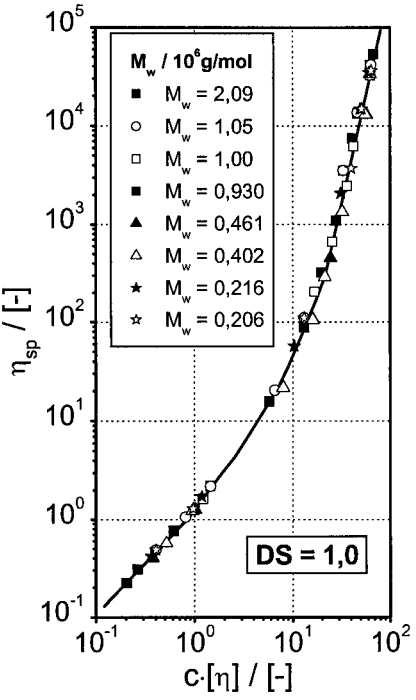

Figure 5. Specific viscosity η_{sp} as a function of the product of concentration c and intrinsic viscosity [η] for carboxymethyl cellulose of different molar masses but the same degree of substitution (DS).

The critical concentration at which this occurs is the reciprocal of the intrinsic viscosity, since the density of a cellulose derivative in solution is directly correlated with $[\eta]$:

$$c^*_{[\eta]} = \rho_{polymer\ in\ solution} \approx \frac{1}{[\eta]} \qquad (6)$$

This theoretical critical concentration depends on the model system chosen (Einstein for example determined a correlation factor for the intrinsic viscosity of 2.5 for the case of hard spheres). Still a comparison of this theoretical critical concentration to an absolute critical concentration calculated from the radius of gyration

$$c^*_{LS} = \frac{m_{polymer\ coil}}{V_{polymer\ coil}} = \frac{M/N_A}{4/3\pi R_G^3} \qquad (7)$$

is an index of how compact the structure of a polymer and how strong the interactions with the solvent and the intermolecular polymer interactions are. Cellulose derivatives show generally large values of $c^*_{[\eta]}/c^*_{LS}$ compared to other polymer solution systems as can be seen in Table 3.

Table 3. The relation of the critical concentration of intrinsic viscosity and the critical concentration from absolute radii of gyration for several aqueous polymer solution systems.

Sample	$c^*_{[\eta]}/c^*_{LS}$
Spheres (Latex, Albumin)	~1
Dextran	4
Pullulan	7
Polystyrene (in Toluene)	10
Polyacrylamide	10
λ-Carrageenane	12
hmHEC	22
Methyl cellulose	25
Carboxymethyl cellulose	28
Methylhydroxyethyl cellulose	35

Distribution Functions

SEC (Size Exclusion Chromatography)

To determine the molar mass distribution of a cellulose derivative, it is first necessary to fractionate the sample into the individual molar masses. Size exclusion chromatography (SEC) has established itself as a powerful method of fractionating polymers.[18,35] Among

the benefits of SEC are the low sample quantities (mg range), a wide separating range (10^3-10^7 g/mol) and short analysis times (1-2 hours).

Separation is carried out on the basis of the hydrodynamic volume of the individual molecules. The separating principle is shown in Figure 6.

When the polymer solution passes through the column system, the molecules can diffuse into all parts of the network to which their size gives them access. Small molecules diffuse more deeply into the gel pores and are retained in the column longer than the larger molecules. Particles that are bigger than the largest pores are not retained at all and are eluted first. The upper limit of fractionation is determined by this size exclusion.[36]

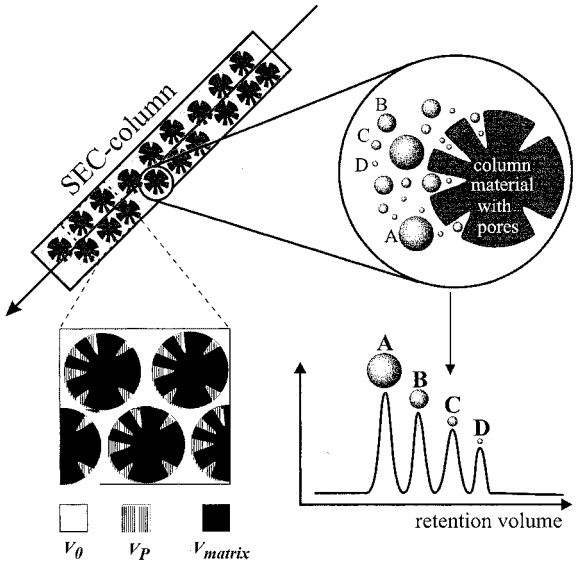

Figure 6. Principle of Size Exclusion chromatography.

The elution volume, V_e, of any particle can be calculated from the following equation:

$$V_e = V_0 + K_{SEC} \cdot V_P \quad (7)$$

where V_e = elution volume; V_0 = interstitial void volume; K_{SEC} = empirical determined distribution coefficient; V_P = pore volume.

$$K_{SEC} = e^{\Delta S^0/R} \quad (8)$$

The measuring results may be distorted by charge effects, such as adsorption or ion exclusion or by degradation of the particle size due to elongation flow forces.

In addition to molecular disperse dissolved chains, solutions of cellulose derivatives also contain aggregates or associates, which can make investigation of the solution difficult or even completely impossible. Often such compounds cannot be investigated with size exclusion chromatography or the associates/aggregates cannot be detected because elongation currents often result in degradation of the associates, or the column acts as a filter which prevents the aggregates from passing.
The detection and fractionation of such superstructures is possible with the aid of field-flow fractionation (FFF).

FFFF (Flow Field-Flow Fractionation)

Separation in flow field-flow fractionation, FFFF, takes place in a channel which in contrast to SEC and other chromatographic methods is only filled with a solvent phase and is therefore not sensitive to adsorption and degradation phenomena on a solid stationary phase. During the separation process a channel flow, $\dot{V}_Z$, with a parabolic flow profile is subjected to a second solvent current (the cross flow, $\dot{V}_X$). The sample constituents are pressed onto the underside of the channel by the cross flow, $\dot{V}_X$. This leads to an increase in concentration which counteracts a back diffusion. The higher the concentration gradient and the greater the diffusion coefficient of a particle is, the greater will be the restoring force. Due to their higher diffusion coefficients, the equilibrium distance of smaller particles is greater than that of larger particles. As a consequence, smaller particles enter faster flow layers of the parabolic flow profile and are removed correspondingly faster.
Two channel types of FFFF are commonly used, the symmetrical version, sFFFF established in the early 60s[37], and the asymmetrical version, aFFFF[38]. The difference between these two is the way the cross flow is applied. With the sFFFF the cross flow is circulating during the fractionation whereas the non-active cross flow of the aFFFF is achieved by a simple elution of the solvent that is constantly withdrawn from the system through the porous bottom plate of the channel. The handling of the aFFFF is easier than the sFFFF and the values are more accurate due to sufficient fractionation. The separation principles of an asymmetric FFFF are shown in Figure 7.

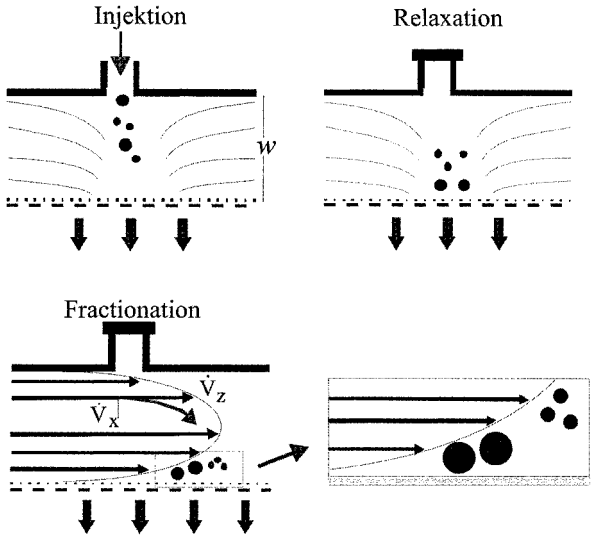

Figure 7. Principle of the asymmetric Flow Field-Flow Fractionation (aFFFF).

As the separation process of FFFF is based on calculable physical processes, the retention volume or retention time of a particle is open to exact theoretical description. Therefore if the channel height, w, is known, the diffusion coefficient, D, can be calculated from the retention time, t_r, according to Eqn. (9).

$$D = \frac{w^2}{6 \cdot t_r} \cdot \frac{\dot{V}_x}{\dot{V}_z} \qquad (9)$$

In dilute solution, the diffusion coefficient is linked with the hydrodynamic radius via the Stokes-Einstein relationship.

$$R_H = \frac{k \cdot T}{6\pi \cdot \eta \cdot D} = \frac{k \cdot T \cdot t_r}{\pi \cdot \eta \cdot w^2} \cdot \frac{\dot{V}_z}{\dot{V}_x} \qquad (10)$$

FFFF can be employed over a large range of molar masses (10^4 - >10^7) and particle sizes (10nm-100μm). Beyond a particle size of approx. 1μm, the separating mechanism is overlapped by steric effects and a reversal in the elution sequence may result as shown in Figure 8.[39]

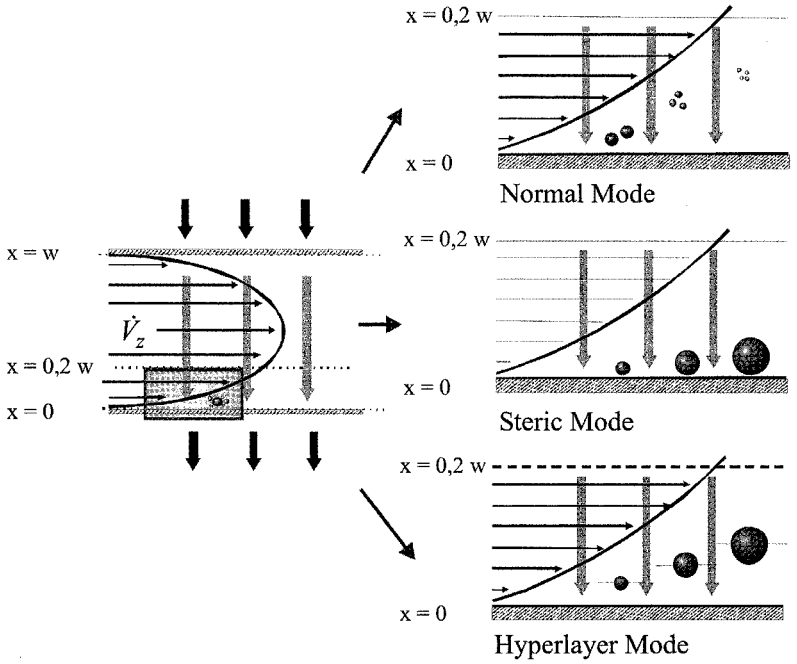

Figure 8. A perfect fractionation occurs if the normal mode of separation is valid. Other possible modes as the steric or hyperlayer modes of FFFF separation can cause problems in the separation.

Hyphenated Techniques

If a fractionating unit is coupled with a concentration detector and additionally with a molar-mass-specific detector, the molar mass and concentration can be determined for every fraction of the sample. This enables the molar mass distribution to be determined absolutely[40,41] as demonstrated in Figure 9 for the hyphenation of either SEC or FFFF with Multi Angle Laser Light Scattering (MALLS) and a differential refractometer (DRI). A first successful combination of FFFF and MALLS was established in the mid-1990s.[16,17,42]

Light scattering is suitable as an absolute method of molar mass detection because the light scattering cell can be operated with continuous flow and online detection is possible. Here the information on molar mass can be obtained immediately as a function of the scattered light intensity. The use of multi-angle laser light scattering (MALLS) photometers has the advantage that information on the radius of gyration, R_G, of molecules greater than $\lambda/20$ can be obtained from the angular dependency of the scattered

light[43]:

$$\frac{K \cdot c}{R_j} = \frac{1}{M} + \frac{16 \cdot \pi^2 \cdot n_0^2}{3 \cdot M \cdot \lambda} \cdot R_G^2 \cdot \sin^2\left(\frac{j}{2}\right) + \ldots \quad (8)$$

with

$$K = \frac{4\pi^2 n_0^2}{N_A \lambda^4} \left(\frac{\mathrm{d}n}{\mathrm{d}c}\right)^2_{p,T,\lambda} \quad \text{and} \quad R_j = \frac{I_j}{I_0} \cdot \frac{h^2}{V_S} \quad (9)$$

The scattered light intensity at an angle j, I_j, enters as a reduced parameter, R_j, which is normalized to the intensity of the incident light beam, I_0, and the distance of the detector, h, from the scattering volume, V_S.

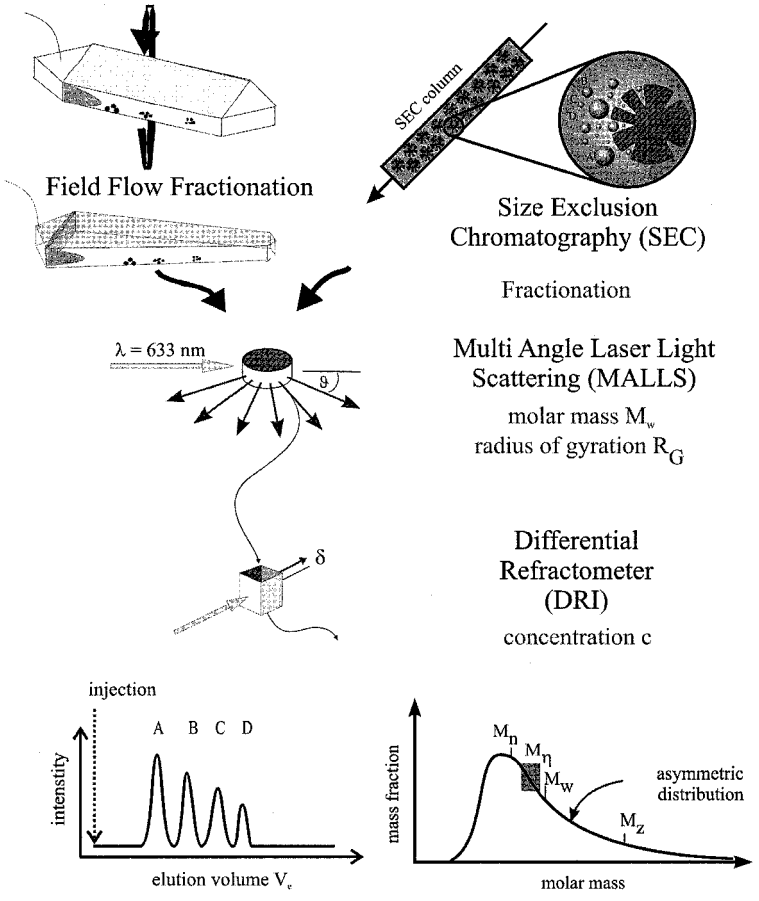

Figure 9. Schematic of hyphenated techniques to simultaneously fractionate and determine molar mass, radius of gyration and concentration of a distributed polymer sample.

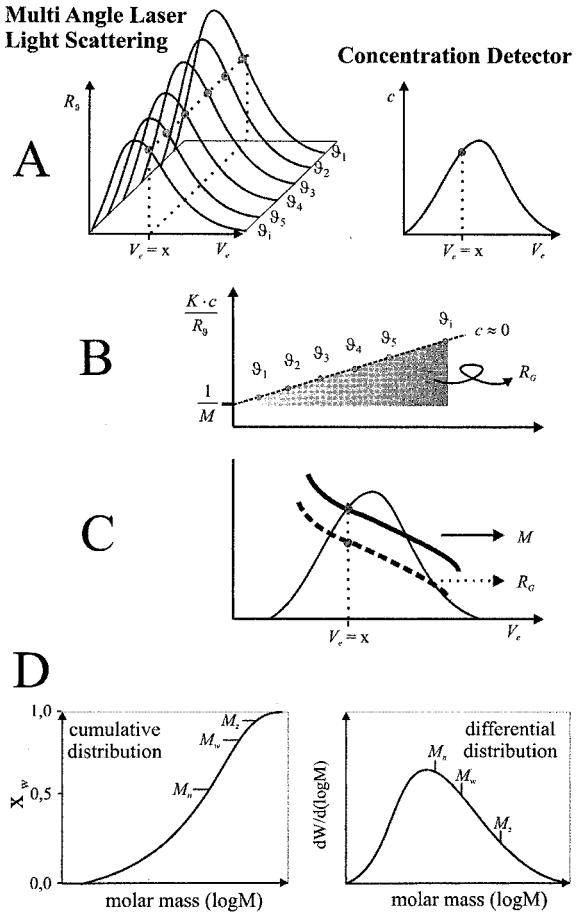

Figure 10. a) Scattered light intensity R_j at different angles j and the concentration c are determined simultaneously for the eluate from the fractionation unit. b) A one-dimensional Zimm graph gives the reciprocal of the molar mass, M_W, at the extrapolated angle $\vartheta=0$. R_G can be obtained from the gradient. c) In this way, the molar mass and radius of gyration can be determined for every fraction and can be plotted as d) the cumulative or differential distribution.

The scattered light intensity depends on the molar mass M as well as on the Radius of Gyration R_G, both values can be extracted from measurements at multiple angles as shown in Figure 10.

The coupling of SEC with MALLS/DRI may be regarded as established whereas coupling FFFF with MALLS/DRI has caused considerable difficulty, which has resulted in the latter technique not being successfully coupled until 1994.[16,17]

Fractionation of Cellulose Derivatives

The determination of the distribution function of cellulose derivatives with the combined technique of SEC/MALLS/DRI is generally possible for isolated polymer coils in solution systems that form no aggregates and are molecular dispers. Figure 11 gives an example for an elution diagram of a hydrophobically modified hydroxyethyl cellulose (hmHEC). Although the hydrophobic modification (hm) of the hmHEC has little effect on the coil dimension, it has a strong influence on the flow behaviour due to enhanced intermolecular interactions of the hm groups.[44] However, in the diluted regime for SEC/MALLS/DRI measurements the hmHEC is molecular disperse in solution. The intensity of the scattered light (here only the signal at an angle of 90° is shown) and the concentration as a function of the elution volume allow the calculation of the molar mass and the radius of gyration as a function of the elution volume.

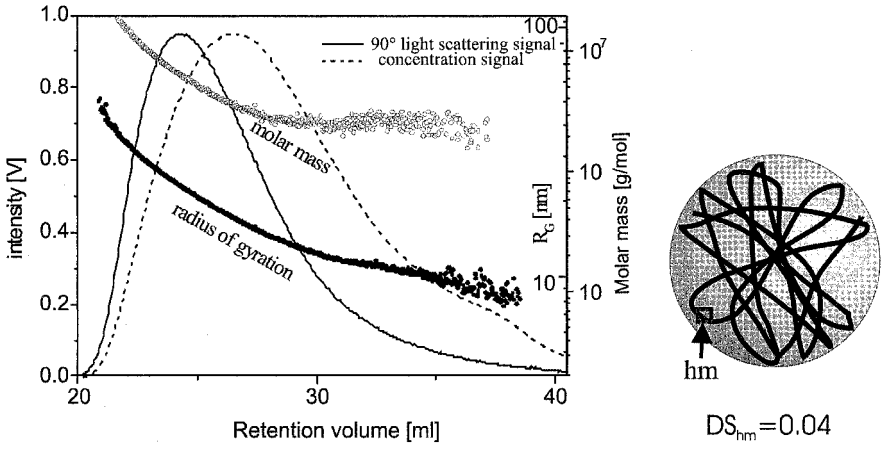

Figure 11. Elution diagram for a hydrophobically (hm) modified hydroxyethyl cellulose (hmHEC) with a DS_{hm}=0,04 in aqueous solution, determined with a hyphenated SEC/MALLS/DRI technique.

This knowledge of the molar mass (or radius of gyration) as a function of the elution volume enables the calculation of the distribution function. Figure 12 gives an example of the molar mass distribution calculated in this way for a hydroxypropyl cellulose (HEC), fractionated in this case via FFFF.

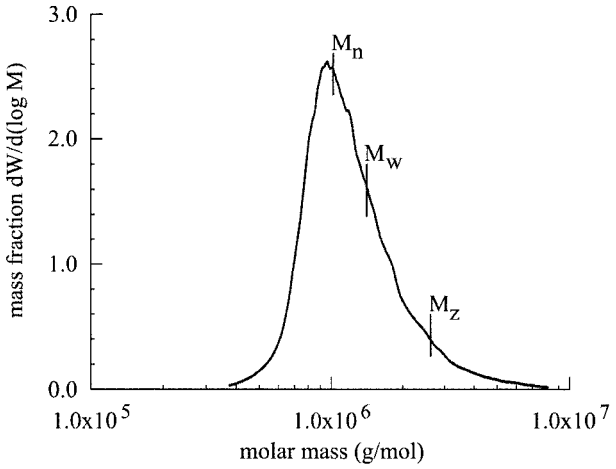

Figure 12. Molar mass distribution for a hydroxyethyl cellulose in 0.1 mol/L $NaNO_3$ determined with a hyphenated FFFF/MALLS/DRI technique.

The advantage of obtaining the whole distribution function rather than just a single average molar mass is shown in Figure 13 for the methylhydroxyethyl cellulose presented in Table 2. The ultrasonic degradation of the polymer leads not only to decreasing average molar masses, but also to a narrowing of the molar mass distribution. However, problems arise if the cellulose derivative solutions contain aggregated or not molecular disperse dissolved structures in the specific solvent.

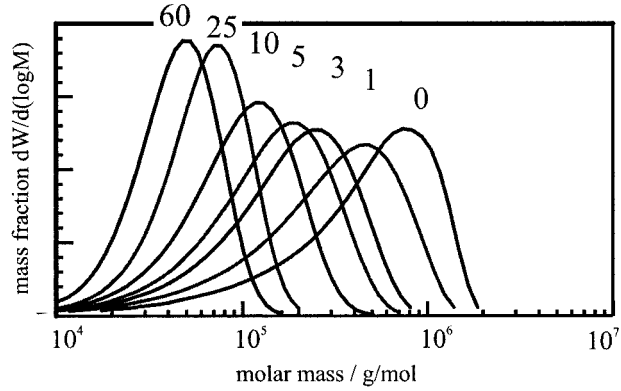

Figure 13. Differential distribution functions of the molar mass of the methylhydroxyethyl celluloses from Table 2 for different degradation times of an ultrasonic degradation . The polydispersity (width of distribution) decreases with time.

In this case these supramolecular structures might not be able to penetrate through the openings between the gel particles in the SEC columns and will not be recovered after the eluate passed through the column. The elution diagram is in these cases misleading, since it is unknown which part of the distributed molar masses is retained in the aggregated structures. It is possible to measure the percentage of polymer that is actually passing through the column. This recovery rate allows to determine the quality of the fractionation and the significance of the obtained distribution functions. Table 4 for example shows the recovery for several different cellulose derivatives after fractionation via SEC.

Table 4. Average molar masses, radius of gyration and recovery for several cellulose derivatives after fractionation via SEC.

Sample	M_W [g/mol]	M_W/M_n	R_{GZ} [nm]	Recovery [wt %]
Methyl cellulose				
MC 1	65,000	2.4	36	94 ± 10
MC 2	183,000	3.9	47	90 ± 10
MC 3	166,000	2.7	48	85 ± 10
MC 4	231,000	4.0	61	84 ± 10
MC 5	351,000	2.2	78	83 ± 10
Methylhydroxyethyl cellulose				
MHEC 1	297,000	2.1	71	99 ± 10
MHEC 2	335,000	2.6	82	98 ± 10
MHEC 3	360,000	2.9	90	92 ± 10
MHEC 4	299,000	2.3	72	87 ± 10
MHEC 5	294,000	2.9	76	72 ± 10
Carboxymethyl cellulose				
CMC 1	176,000	3.2	60	96 ± 10
CMC 2	375,000	2.9	95	95 ± 10
CMC 3	839,000	1.4	135	42 ± 10

For low recovery rates, the distribution function is likely to underpredict the share of high molar mass polymer that are caught in the aggregates and separated from the eluate by the column. However, since the composition of the aggregated structures is unknown, the interpretation of distribution function of aggregated systems obtained from SEC fractionation is difficult.

For the fractionation of aggregated systems, FFFF is more suitable, since there is no filling material in the channel that can filter out the larger aggregate particles. In this it is possible

to determine the molar mass even for partially aggregated systems as demonstrated for a hydroxypropyl cellulose in Figure14.

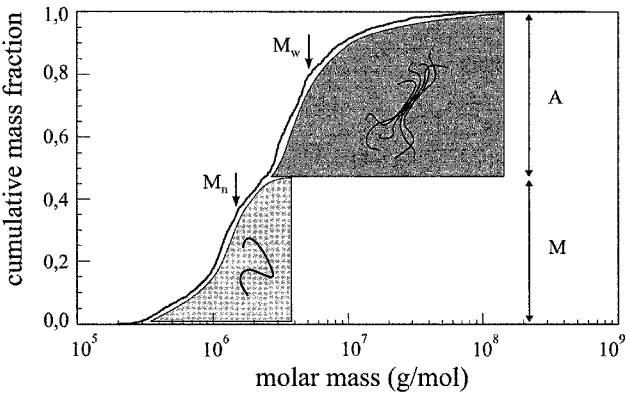

Figure 14. Cumulative distribution of the molar mass of a hydroxypropyl cellulose determined with FFFF/MALLS/DRI. *A* indicates the aggregated part of the polymers, *M* the molecular disperse fraction.

The cumulative distribution function in Figure 14 shows two neatly separated fractions. The high molar mass fraction has a much larger mass than one would expect for single molecules of a hydroxypropyl cellulose and is much likely to consist of aggregated clusters of two and more polymer molecules.

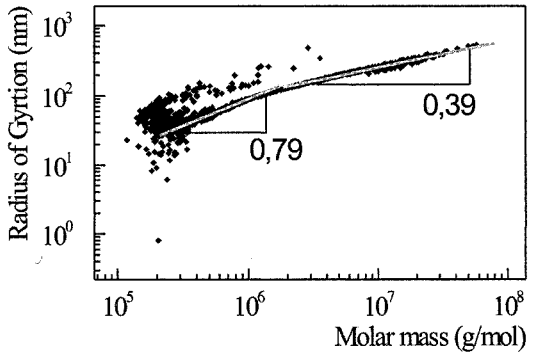

Figure 15. Radius of gyration R_G as a function of the molar mass *M* for the HPC from Figure 14.

This is backed up by the dependence of the radius of gyration from the molar mass in Figure 15. As already pointed out, the exponent ν of the R_G-M-relationship (Eq. (3)) and therefore the slope in the double logarithmic plot of Figure 15 is a measure of how compact the structure of the polymer molecules in the solution is. The small slope of 0.39 at high molar masses indicates that this fraction is very likely to have a much more compact internal structure as expected for aggregated clusters of multiple polymers.

[1] M. Eggersdorfer, S. Warwel, G. Wulff, "*Nachwachsende Rohstoffe - Perspektiven für die Chemie*". VCH, Ludwigshafen, Aachen 1993.
[2] D. Klemm, B. Philipp, T. Heinze, U. Heinze, W. Wagenknecht, "*Comprehensive Cellulose Chemistry*". Vol. 1. Wiley-VCH, Weinheim 1998.
[3] H. Krässig, J. Schurz, R. G. Steadman, K. Schliefer, W. Albrecht, in "*Ullmann's Encyclopedia of Industrial Chemistry*", 5, W. Gerhartz, Editor. 1992, Wiley VCH, Weinheim, p. 375.
[4] R. D. Gilbert, ed. *Cellulosic Polymers*. 1994, Carl Hanser Verlag: München.
[5] W. Burchard, ed. *Polysaccharide - Eigenschaften und Nutzung, Eine Einführung*. 1985, Springer: Freiburg.
[6] Y. L. Meltzer, "*Water-Soluble Polymers - Developments since 1978*", Chemical Thechnology Review. Vol. 181. NDC, New Jersey 1981.
[7] W. M. Kulicke, O. Arendt, M. Berger, *Colloid Polym. Sci.* **1998**, *276*, 1019.
[8] H. A. Shelanski, A. M. Clark, *Food Res.* **1948**, *13*, 29.
[9] W. Kern, *Pharm. Ind.* **1959**, *21*, 45.
[10] Y. Pomeranz, "*Functional Properties of Food Components*", 2 ed. Academic Press, San Diego 1991.
[11] W. M. Kulicke, M. Otto, A. Baar, *Macromol. Chem. Phys.* **1993**, *194*, 751.
[12] N. Schittenhelm, W. M. Kulicke, *Macromol. Chem. Phys.* **2000**, *201*, 1976.
[13] W. M. Kulicke, D. Roessner, W. Kull, *Starch-Starke* **1993**, *45*, 445.
[14] M. Mueller, *Preparation of polytetramethylene ether glycol diester using an aluminosilicate type catalyst*. 1994, PCT (Shinwha Engineering and Construction Co. Ltd., S. Korea). p. 22 pp.
[15] W. M. Kulicke, M. Otto, A. Baar, *Makromol. Chem.-Macromol. Chem. Phys.* **1993**, *194*, 751.
[16] D. Roessner, W. M. Kulicke, *J. Chromatogr. A* **1994**, *687*, 249.
[17] H. Thielking, D. Roessner, W. M. Kulicke, *Analytical Chemistry* **1995**, *67*, 3229.
[18] J. Klein, W.-M. Kulicke, J. Hollmann, in "*Analytiker Taschenbuch*", H. Günzler, Editor. 1998, Springer, Berlin, p. 317.
[19] W.-M. Kulicke, C. Clasen, "*Viscosimetry of Polymers and Polyelectrolytes*". Springer, Heidelberg 2004.
[20] J. Brandrup, E. H. Immergut, "*Polymer Handbook*", 4 ed. John Wiley & Sons, New York 1999.
[21] C. Clasen, W. M. Kulicke, *Prog. Polym. Sci.* **2001**, *26*, 1839.
[22] W.-M. Kulicke, "*Fließverhalten von Stoffen und Stoffgemischen*". Hüthig und Wepf, Basel, Heidelberg, New York 1986.
[23] W. Schnabel, "*Polymer Degradation. Principles and Practical Application.*" Carl Hanser Verlag, München 1981.
[24] P. Pfefferkorn, J. Beister, A. Hild, H. Thielking, W.-M. Kulicke, *Cellulose (Dordrecht, Netherlands)* **2003**, *10*, 27.
[25] W. M. Kulicke, *Chemie Ingenieur Technik* **1986**, *58*, 325.
[26] W. M. Kulicke, R. Kniewske, R. J. Muller, M. Prescher, H. Kehler, *Angew. Makromol. Chem.* **1986**, *142*, 29.
[27] M. Bouldin, W. M. Kulicke, H. Kehler, *Colloid Polym. Sci.* **1988**, *266*, 793.
[28] A. R. Peacocke, N. J. Pritchard, *Biopolymers* **1968**, *6*, 605.
[29] N. J. Pritchard, D. E. Hughes, A. R. Peacocke, *Biopolymers* **1966**, *4*, 259.
[30] M. Okuyama, T. Hirose, *Kolloid Z. Z. Polymere* **1968**, *226*, 70.
[31] G. Gooberman, J. Lamb, *J. Polym. Sci.* **1960**, *42*, 35.
[32] A. M. Basedow, K. H. Ebert, *Adv. Polym. Sci.* **1977**, *22*, 83.
[33] M. Marx-Figini, *Angew. Makromol. Chem.* **1997**, *250*, 85.
[34] W. M. Kulicke, A. H. Kull, W. Kull, H. Thielking, J. Engelhardt, J. B. Pannek, *Polymer* **1996**, *37*, 2723.

[35] D. Heins, W. M. Kulicke, P. Kauper, H. Thielking, *Starch-Starke* **1998**, *50*, 431.
[36] H. G. Barth, *J. Chromatogr. Sci.* **1980**, *18*, 409.
[37] J. C. Giddings, *Separation Science* **1966**, *1*, 73.
[38] K. G. Wahlund, J. C. Giddings, *Analytical Chemistry* **1987**, *59*, 1332.
[39] H. Thielking, W. M. Kulicke, *J. Microcolumn Separations* **1998**, *10*, 51.
[40] S. Lange, D. Heins, W. M. Kulicke, *Abstr. Pap. Am. Chem. Soc.* **1997**, *214*, 66.
[41] W. M. Kulicke, S. Lange, D. Heins, *ACS Symp. Ser.* **1999**, *731*, 114.
[42] H. Thielking, W. M. Kulicke, *Analytical Chemistry* **1996**, *68*, 1169.
[43] U. Adolphi, W. M. Kulicke, *Polymer* **1997**, *38*, 1513.
[44] M. Laschet, J. P. Plog, C. Clasen, W. M. Kulicke, *Colloid Polym. Sci.* **2004**, *282*, 373.